Low-temperature oxidation of carbon monoxide and methane over alumina and ceria supported platinum catalysts

Per-Anders Carlsson *and Magnus Skoglundh

Department of Chemical and Biological Engineering and Competence Centre for Catalysis, Chalmers University of Technology, SE-412 96 Göteborg, Sweden

Abstract

The ignition- and extinction processes for total oxidation of CO, CH_4 and $CO+CH_4$ mixture in oxygen excess over Pt/Al_2O_3 and Pt/CeO_2 catalysts with the platinum phase distributed either homogeneously or heterogeneously (i.e., locally high platinum concentration) in the support have been studied by temperature programmed oxidation experiments. Following the preparation methods by Arnby *et al.* [*J. Catal.* **221** (2004) 252-261], the samples have the same Pt load and dispersion. Generally the catalytic activity follows the order: Pt/CeO_2 (heterogeneous)>Pt/CeO_2 (homogeneous)>Pt/Al_2O_3 (heterogeneous)> Pt/Al_2O_3 (homogeneous) as indicated by lower ignition- and/or extinction temperatures. For Pt/Al_2O_3, the addition of NO_2 to the reactant stream increases the rate of oxidation of CO in the pre-ignition regime although the light-off temperature T_{50} is shifted towards higher temperatures (except for low CO concentrations). In the case of the Pt/CeO_2, the CO conversion generally decreases. For CH_4 oxidation in the presence of NO_2, the conversion increases for Pt/Al_2O_3 and decreases for Pt/CeO_2. The addition of CO_2 in the reactant stream has minor influence on CO oxidation over Pt/Al_2O_3 while for Pt/CeO_2, T_{50} is shifted towards higher temperatures. For the simultaneous oxidation of CO and CH_4, a reverse hysteresis for methane oxidation is observed, i.e., the extinction process occurs at higher temperature than the corresponding ignition process. The improved activity for CO oxidation over samples with heterogeneous Pt distribution is likely due to less tendency towards CO self-poisoning through the development of steeper concentration gradients in the Pt containing regions in the porous support material. The significant increase of activity for both reactions over ceria-supported Pt is here assigned to highly active sites at the platinum-ceria boundary but also, to some extent, the oxygen storage- and release function and dynamics of the transport of oxygen in the Pt/CeO_2 system.

Key words: catalytic ignition; catalytic extinction; metal-support interactions; diffusion

1. Introduction

The catalytic oxidation of carbon monoxide (CO) and hydrocarbons (HC) are key reactions in many industrial chemical processes as well as pollution control for automotives and industrial processes [1]. Within the automotive sector, CO and HC present in the engine exhausts are often efficiently converted to carbon dioxide and water by complete oxidation over monolith catalysts, typically, noble metals supported on metal oxides, mounted in the exhaust system [2,3]. Occasionally, however, obstacles associated with blocking of catalytic sites by the reactants at low temperatures, so-called self-poisoning, results in poor catalytic performance leading to, for example, high cold-start emissions [2–4]. In this connection self-poisoning has often been considered a transient ignition problem mainly solved by strategies for rapid warm-up of the catalysts [5]. This view, however, is about to change. The present development towards more efficient engine combustion concepts, e.g., homogeneous charge compression ignition (HCCI) combustion, leads to low-temperature exhausts ($\sim150°C$ for significant periods) with considerable levels of CO and HC including methane (CH_4) [6,7]. Thus the need for catalysts that are active for continuous operation at low temperatures is increasing.

It is well known that the oxidation of CO on platinum at low pressures exhibits two distinct kinetic regimes, one CO self-poisoned region with low activity and one regime where the surface is predominantly covered with chemisorbed oxygen resulting in high activity [8,9]. Depending on reaction conditions, i.e., temperature and reactant concentrations, the two regimes may overlap forming a region with bistable

---

kinetics. Thus, in the bistable region, the kinetics is not only dependent on the actual reaction conditions but also the reaction history [9–11]. The same phenomena may occur also for supported Pt crystallites at atmospheric pressures [12–15] although the kinetics may be further complicated by, e.g., strong metal-support interactions (SMSI) [16,17], adsorbate diffusion over metal-support boundaries [18,19] and oxide formation [20,21].

Catalytic oxidation of saturated hydrocarbons, and especially methane, is considerably more difficult than oxidation of other hydrocarbons or oxygenates with the same carbon chain lengths. In the case of CH_4 this is reflected by the relatively high temperatures required for the catalytic oxidation to proceed. The rate-limiting step is considered to be the abstraction of the first hydrogen [22], which in terms of catalysis means the dissociative adsorption of CH_4. On Pt, the sticking coefficient is relatively low compared to that of higher alkanes [23] hence the overall methane oxidation rate is also relatively low. In contrast to CO oxidation, oxidation of saturated hydrocarbons and specifically methane over platinum catalysts may suffer from oxygen poisoning [14,24,26–29] leading to low reaction rates [30,31]. Improving the low-temperature activity for simultaneous oxidation of CO and CH_4 over supported Pt is thus a dilemma. In the case of CO oxidation the key issue is to facilitate oxygen supply to the Pt crystallites, while for oxidation of CH_4 an efficient oxygen supply may lead to oxygen poisoning.

One strategy to promote oxidation of CO/CH_4 is to deliberately facilitate the transport of oxygen to/from Pt by appropriate choice of the support material. For example in three-way catalysis, ceria provides oxygen, which is stored under oxidizing conditions, for the conversion of CO and HC under reducing conditions [32–34]. Ceria is also considered to promote the water-gas-shift reaction [35] and promote noble metal dispersion [36,37]. For Pt catalysts it has been shown that using ceria (CeO_2), instead of silica (SiO_2) or alumina (Al_2O_3), as supporting material significantly can improve the activity for CO oxidation [38,39]. Recent results [40] and in particular this study, show that the use of ceria can improve also the activity for oxidation of CH_4. In another strategy to improve CO oxidation over Pt/Al_2O_3 monolith catalysts at low-temperatures, Arnby et al. [26,42] demonstrated an interesting concept based on heterogeneous distribution (local high concentration) of Pt in the alumina support. For such catalysts primarily the extinction of CO oxidation shifted towards lower temperatures thus widening the ignition-extinction hysteresis as compared to the corresponding conventional catalysts with homogeneous Pt distribution in the support material. The mechanisms behind these observations were thoroughly discussed in terms of difference in mass transfer resulting in less CO self-poisoning, difference in heat transfer leading to locally hot regions and a structure sensitive reaction dependent on the local Pt load. In principle, assuming that heat transfer is the main cause, heterogeneous Pt distribution may facilitate also CH_4 oxidation as, generally, reaction rates increase (exponentially) with temperature.

The present study concerns the total oxidation of CO, CH_4 and $CO+CH_4$ mixture with oxygen over Pt/Al_2O_3 and Pt/CeO_2 monolith catalysts. Specifically, the influence of distribution of the active phase in the catalyst layer and choice of support material on the ignition- and extinction processes are studied by temperature programmed oxidation experiments. The effects of NO_2 and CO_2 on these processes are also studied.

2. Experimental section

2.1. *Catalyst preparation and characterisation*

Four different types of supported Pt catalysts were prepared and characterised in terms of apparent total Pt surface area. Following the preparation methods by Arnby et al. [42], catalysts with either homogeneous or heterogeneous distribution of the Pt in the support material were prepared using either alumina or ceria as support material. The main steps in the preparation methods are summarised below.

2.1.1. *Pt/Al₂O₃ and Pt/CeO₂ powder catalysts*
The alumina supported Pt samples were prepared by impregnating alumina (Puralox S Ba 200, particle diameter 45 μm, Sasol Germany GmbH) that has been precalcined in air at 600°C for 2 h with a halogen-free platinum precursor. Alumina was dispersed in distilled water, and an aqueous solution of $Pt(NO_3)_2$ (W. C. Heraeus GmbH & Co. KG) was added dropwise to the alumina slurry under continuous stirring. The slurry was thereafter instantly frozen with liquid nitrogen and freeze-dried. The resulting powder was calcined in air at 600°C for 1.5 h. The corresponding ceria supported Pt samples were prepared analogously using ceria (99.5 HA514, particle size 10-20 nm, Rhône-Poulenc) instead. Two different Pt loadings, i.e., 1 and 10 wt.-%, were prepared for each support material.

2.1.2. *Monolith catalysts with homogeneous and heterogeneous Pt distribution*
Monolith samples (length=15 mm, ∅=12 mm) were cut out from a commercial honeycomb structure with 400 cpsi. The Pt/Al_2O_3 monolith catalyst with homogeneous Pt distribution was prepared by immersing the monolith body into a well stirred washcoat slurry consisting of the 1 wt.-% Pt/Al_2O_3 powder (75% of the total support content), boehmite sol (Disperal sol P2, particle size 25 nm, Condea) and distilled water. The sample was dried in air at 100°C for 2 min and calcined, also in air, at 600°C for 3 min. This procedure was repeated until 200 mg of washcoat was applied on the monolith. This correspond to 0.12 g coating per cm^3 monolith catalyst. The sample was then finally calcined in air at 600°C for 2 h. The Pt/Al_2O_3 catalyst with heterogeneous Pt distribution was prepared analogously using instead a washcoat slurry consisting of the 10 wt.-% Pt/Al_2O_3 powder (7.5% of the total support

Table 1
Summary of reaction conditions. The heating/cooling ramp rate was $5°C/min$ and the temperature was kept constant for 10 min at the highest and lowest temperatures.

Thermal sequence [°C]	Feed gas composition
350→50→350	0.1%CO + 9%O_2
"	1%CO + 9%O_2
"	0.1%CO + 9%O_2 + 0.03% NO_2
"	1%CO + 9%O_2 + 0.03% NO_2
"	0.1%CO + 9%O_2 + 5% CO_2
"	1%CO + 9%O_2 + 5% CO_2
550→50→550	0.05%CH_4 + 9%O_2
	0.05%CH_4 + 9%O_2 + 0.03%NO_2
"	1%CO+ 0.05%CH_4 + 9%O_2

content), alumina, boehmite sol and distilled water. The Pt/CeO_2 monolith catalysts were prepared accordingly using in the case of homogeneous Pt distribution a washcoat slurry consisting of 1 wt.-% Pt/CeO_2 powder (75% of the total support content), ceria sol (CeO_2 (ACT), particle size 10-20 nm, Nyacol Nano Technologies, Inc.) and distilled water, and in the case of heterogeneous Pt distribution a slurry of the 10 wt.-% Pt/CeO_2 powder (7.5% of the total support content), ceria, ceria sol and distilled water. The apparent Pt surface area was characterised by the amount of adsorbed CO which was determined by temperature programmed CO desorption experiments. The adsorbed amount of CO for the respective catalyst was 1.35 (homogeneous Pt/Al_2O_3), 1.30 (heterogeneous Pt/Al_2O_3, 0.5 (homogeneous Pt/CeO_2) and 1.48 (heterogeneous Pt/CeO_2) μmol per monolith catalyst. For the alumina samples, the obtained values are close while for the ceria samples the values are diverging especially for the homogeneous Pt/CeO_2 sample. In contrast to alumina-based catalysts, the determination of noble metal dispersion on ceria-based samples is not straightforward due to the inherent properties of the platinum-ceria system, e.g., adsorption/desoprtion phenomena on the ceria phase, redox behaviour and spillover mechanisms [43]. Thus we consider the present values obtained for the Pt/CeO_2 catalysts as indications rather than precise measures of the apparent Pt surface area.

2.2. Catalyst activity measurements

2.2.1. Continuous gas flow-reactor design
The CO oxidation experiments were carried out using a continuous gas-flow reactor as described elsewhere [44]. Briefly, it consists of a horizontal quartz tube (L=600 mm, $\varnothing$= 15 mm) surrounded by a metal coil for resistive heating. The quartz tube and heating coil were carefully insulated. Two thermocouples (Reckman type K) were used to measure, respectively, the inlet gas temperature 11 mm upstream of the front of the sample and the catalyst temperature in the center of the monolith body. The inde-

pendent inlet gas temperature was used for temperature control via a standard PID regulator (Eurotherm). Gases were introduced to the reactor via individual mass flow controllers (Bronkhorst Hi-Tech). The product stream was analysed on-line with respect to CO and CO_2 concentrations using non-dispersive infrared analysers (UNOR 6N, Maihak). Analogous to the CO oxidation experiments, the methane oxidation experiments were carried out using a similar continuous gas-flow reactor set-up [27]. In this case, however, the product stream was continuously analysed by mass spectrometry (Balzers Quadstar 422) following the m/z ratios 2 (H_2), 15 (CH_4), 18 (H_2O), 28 (CO), 32 (O_2) 40 (Ar) and 44 (CO_2).

2.2.2. Temperature programmed oxidation experiments
The influence of the Pt distribution and the support material on the ignition- and extinction processes for oxidation of CO, CH_4 and CO+CH_4 mixture, respectively, were studied by temperature programmed oxidation (TPO) experiments using heating/cooling ramps of $5°C/min$ and constant feed gas composition. This heating/cooling ramp rate allowed for two data acquisitions per °C. Special attention was paid to the influence of NO_2 on the ignition- and extinction processes for CO and CH_4 oxidation. Also the influence of CO_2 on the CO oxidation was studied. Generally the experiments were carried out such that the extinction process was first studied followed by the ignition process. For the CO oxidation experiments the total gas flow was 1500 ml/min (NTP) corresponding to a space velocity of about 75000 h^{-1} (N_2 as balance). In all experiments with CH_4 and CO+CH_4 mixture, the total gas flow was 400 mL (NTP)/min corresponding to a space velocity of 20000 h^{-1} (Ar as balance). For all experiments, the thermal sequence and feed gas composition, are summarised in Table 1.

3. Results and discussion

3.1. Oxidation of CO

Figure 1 shows the results from TPO of 0.1 and 1% CO over homogeneous (top panel) and heterogeneous (bottom panel) Pt/Al_2O_3 during heating-cooling ramps. In Table 2 the temperatures corresponding to 50% reactant conversion for all ignition- and extinction experiments are summarised. In the ignition experiments, the CO conversion follows a typical light-off process for oxidation of CO over platinum, which occurs through three main phases. The first phase describes the situation at low CO conversions. In this phase, the competitive adsorption of CO and O_2 favors CO adsorption to such an extent that the reaction is CO self-poisoned [13]. Thus the CO conversion is low and the reaction is kinetically controlled. Next phase covers intermediate conversions. Here the reaction rate becomes controlled by internal diffusion in the porous support material of the catalyst, thus turning from the first to the second phase means a shift in rate-determining step (RDS).

According to Weisz and Prater [45], internal diffusion will affect a first-order reaction for values of the Weisz modulus (Φ) equal or higher than one. Conservatively first-order reactions will be kinetically controlled for $\Phi < 0.6$ [46]. Reactions with negative reaction orders, like CO oxidation over platinum in the CO self-poisoned regime, are influenced by internal diffusion if $\Phi \geq |n|^{-1}$ [47]. In the present case the transition from the kinetically to the diffusion controlled regime is estimated to occur at about 20% CO conversion ($\Phi = 0.6$). This conversion limit is likely overestimated as in the present calculation, the observed reaction rate is related to the entire catalyst layer, which may not be the case. Thus the second phase may here include both the catalytic ignition and light-off processes. In Figure 1, the catalytic ignition occurs at temperatures corresponding to CO conversions slightly below 20%. Strictly, the ignition temperature is a critical point defined by the Frank-Kamenetskii criterion [48], at which the increase in exothermic heat flux from the reaction exceeds the increase in heat loss flux. This leads to a self-acceleration of the reaction rate [48,49] towards and beyond the light-off temperature (here defined as the temperature for which 50% reactant conversion is achieved). The catalytic ignition is thus a heat balance and kinetics problem. Finally, the third phase concerns complete conversions, i.e., temperatures well above the light-off region [50]. Entering this phase means, again, a shift in RDS as here the reaction rate becomes controlled by external (gas phase) diffusion. Analogously, the extinction experiments means the reversed transition from the third to the first phase. In general, the extinction process occurs at considerably lower temperatures than the corresponding ignition process demonstrating a clear ignition-extinction hysteresis. This is partly due to inherent kinetic bistability (see Introduction) and the interplay between reaction kinetics and diffusion phenomena, and partly caused by a heat effect, i.e., exothermic reaction heat generated at the ignition point heats the catalyst so that the inlet gas temperature can be decreased below the temperature required for ignition without influencing the reaction rate significantly [48,49].

From Figure 1 and Table 2, it is clear that both the ignition and extinction processes are shifted towards lower temperatures for the catalyst with heterogeneous Pt distribution as compared to the homogeneous Pt/Al$_2$O$_3$ sample. Also, in the case of 0.1% CO, the ignition-extinction hysteresis is significantly broader for the heterogeneous sample which essentially is due to a shift of the extinction process from around 145°C (homogeneous Pt/Al$_2$O$_3$) to around 127°C. These results are in agreement with previous studies [26,42] in which the impact of Pt distribution on the activity for CO oxidation was discussed in terms of difference in mass transfer, difference in heat transfer, and structure of the active phase. Although difference in mass transfer was pointed out as the most likely cause to the observed effects, the influence of a structure sensitive reaction could not be completely ruled out. Carefully considering the CO conversion profiles in the second phase, i.e., intermediate conver-

Table 2
Summary of temperatures corresponding to 50% reactant conversion for the ignition (light-off) and extinction processes over homogeneous and heterogeneous Pt/Al$_2$O$_3$ and Pt/CeO$_2$ catalysts studied by temperature programmed oxidation using heating/cooling rate of 5°C/min.

| Gas composition | Homogeneous Pt/Al$_2$O$_3$ | | | Heterogeneous Pt/Al$_2$O$_3$ | | | Homog | |
(N$_2$-Ar mixture as carrier)	T$_{ign}$	T$_{ext}$	ΔT	T$_{ig}$	T$_{ex}$	ΔT	T$_{ig}$	T$_e$
0.1% CO	170	145	25	164	127	37	-	-
1% CO	234	176	58	226	169	57	143	10
0.05% CH$_4$	-	-	-	-	-	-	359	35
1% CO + 0.05% CH$_4$, CO:	235	180	55	245	185	60	198	16
1% CO + 0.05% CH$_4$, CH$_4$:	-	-	-	-	-	-	422	50
0.1% CO + 0.03% NO$_2$	183	171	12	162	148	14	182	15
1% CO + 0.03% NO$_2$	250	209	41	232	192	40	192	16
0.1% CO + 5% CO$_2$	176	151	25	166	128	38	162	14
1% CO + 5% CO$_2$	240	179	61	230	170	60	171	13
0.05% CH$_4$ + 0.03% NO$_2$	-	-	-	-	-	-	510	50

sions including the ignition and light-off processes, one can observe that in the case of heterogeneous Pt/Al$_2$O$_3$, the increase in CO conversion through the ignition point is more smooth than for the sample with homogeneous Pt distribution. Also the increase in CO conversion during light-off is somewhat slower (slope less steep) in the case of heterogeneous Pt/Al$_2$O$_3$. As the reaction rate in this phase is controlled by internal diffusion, these observations suggest that for heterogeneous Pt/Al$_2$O$_3$, diffusion in the catalyst layer plays a more pronounced role. This can be understood by considering the difference in Pt distribution. During ignition over the heterogeneous Pt/Al$_2$O$_3$ sample, local concentration gradients in the Pt containing regions of the catalyst layer develop at lower CO conversions as in these regions the Pt density is higher as compared to the homogeneous Pt/Al$_2$O$_3$ catalyst. This results in less CO self-poisoning and thus ignition occurs at lower temperatures. For the same reasons, i.e., more pronounced concentration gradients, the extinction process is shifted towards lower temperatures for the heterogeneous Pt/Al$_2$O$_3$ sample. This is especially clear in the case of 0.1% CO because thermal effects through reaction exothermicity are considerably lower than in the case of 1% CO. Here one may note that complete oxidation of 0.1% CO at adiabatic conditions leads to a temperature increase of about 10°C while the corresponding oxidation of 1% CO increases the temperature further one order of magnitude.

Figure 2 shows the ignition- and extinction experiments for homogeneous and heterogeneous Pt/CeO$_2$ catalysts, analogous to the experiments with Pt/Al$_2$O$_3$ catalysts described above. It is clear that ceria as support material significantly improves the oxidation activity. The light-off temperature for oxidation of 1% CO occurs at temperatures almost 100°C lower than for the corresponding Pt/Al$_2$O$_3$ catalysts. In addition, significant conversion is achieved even at 50°C, the lowest temperatures studied here, especially in the case of 0.1% CO for which no less than about 30% and 40% conversion is achieved for, respectively, the heterogeneous and homogeneous Pt/CeO$_2$ catalyst. Al-

though the conversion of CO below light-off is higher in the case of homogeneous Pt/CeO_2, the heterogeneous Pt/CeO_2 catalyst reaches light-off at about 20°C lower temperature. Interestingly, the width of the ignition-extinction hysteresis is similar and the conversion of CO passes through a minimum during the ignition- and extinction experiments for both catalysts.

To efficiently utilise noble metals, ceria can be used as support to achieve high precious metal dispersion, thereby achieving high activity per mass of metal [36,37]. In this study, such dispersion effects are expected to be minor as the apparent platinum dispersion for the present catalysts is deliberately similar. We recall that the differences in CO uptake of the ceria catalysts may be due to the inherent properties of the Pt/CeO_2 system and thus not solely indicative of varying Pt dispersions [43]. In ceria, Ce is well known to have the ability to readily change oxidation state ($Ce^{4+} \leftrightarrow Ce^{3+}$) thereby provide a function as an oxygen storage- and release material [51]. Moreover ceria can facilitate transport of oxygen mainly through surface diffusion but also via bulk diffusion at sufficiently high temperatures (above 400°C [52]). Thus, in the case of CO oxidation over Pt/CeO_2 catalysts, ceria has been suggested to provide an additional channel for transport of oxygen to the Pt crystallites through reversed spill-over, i.e., oxygen diffusion from the ceria support to the Pt crystallites [38,39], thereby supress the effect of CO self-poisoning. This can partly explain the present results. However, the ignition- and extinction processes observed here occur well below 150°C. At these temperatures, transport of oxygen in the ceria bulk is negligible and surface diffusion is likely minor [52] which suggests that also other mechanisms may be important. For example, in contrast to the Pt/Al_2O_3 catalyst, platinum supported on ceria may exhibit SMSI [16] and connected to this, ceria as support may result in electronic promotion of the Pt crystallites or exclusive active sites at the platinum-ceria boundary [40,53] favoring the CO oxidation. The latter may favor processes like CO spill-over, O_2 dissociation or give rise to more oxidised Pt species at the boundary, through reversed oxygen spill-over [54], for which the adsorption of CO is weak. In all these cases the boundary sites are expected to be less sensitive towards CO poisoning. We mention that the oxidation of CO on bare ceria has been reported to be minor at these temperatures [55]. The further improvement of the CO oxidation activity for heterogeneous Pt/CeO_2 is then likely due to the effect of heterogeneous Pt distribution analogous to the case of Pt/Al_2O_3 discussed above. The peculiar minimum in CO conversion is more difficult to explain. For example, CO adsorption/desorption phenomena that lead to a net accumulation/release may cause an apparent minimum in CO conversion. This explanation, however, seems less likely. The detailed analysis of the carbon balance ($CO+CO_2$) reveals negligible carbon accumulation at low temperatures or, in other words, the amounts of produced CO_2 corresponds well with the consumed amounts of CO. Considering this, we can only speculate on the un-

derlying phenomena. For example during the change of the temperature the mobility of surface species is also changed possibly leading to a rearrangement of adsorbed CO from ceria to platinum sites. This can result in a temporary low activity in the pre-ignition regime.

The influence of NO_2 and CO_2 on the ignition- and extinction processes was studied as well. In Figure 3 and 4, the results from CO oxidation in the presence of 0.03% NO_2 for, respectively, the Pt/Al_2O_3 and Pt/CeO_2 catalysts, are shown. The corresponding results for CO_2 addition are only shown in Table 2. Addition of NO_2 clearly shifts the ignition- and extinction processes towards higher temperatures for all catalysts. In the case of 1% CO, the light-off temperature is shifted about 20°C for Pt/Al_2O_3 and 50°C for Pt/CeO_2. The extinction process in the respective case is shifted even more leading to narrower ignition-extinction hysteresis. The results for 0.1% CO is similar, however, for the Pt/Al_2O_3 catalysts, NO_2 addition significantly increases the CO conversion below the ignition temperature. Addition of CO_2 has a minor influence on the CO oxidation over Pt/Al_2O_3 while for the Pt/CeO_2 catalyst the ignition- and extinction processes are shifted about 30°C towards higher temperatures.

At the temperatures studied here, a less active oxide-like platinum phase can be formed during CO oxidation over Pt/Al_2O_3 [14], especially in the presence of NO_2. Experiments with NO_2 pre-treated Pt/Al_2O_3 subsequently exposed to CO support this [14]. Although the detailed mechanism/characteristics of the oxide formation is not clear, models based on a nucleation process followed by growth of oxide islands have been suggested [21]. In the case of Pt/Al_2O_3, the observed shift of the ignition- and extinction processes towards higher temperatures can thus be due to formation of a platinum oxide phase slightly after the ignition point where the CO coverage is low. The increased CO conversion before light-off that is observed only for the lowest level of CO (0.1%) where the CO poisoning is less severe, is likely due to dissociation of NO_2 on the (few) available free sites not accessible for O_2 dissociation. An alternative explanation may involve an Eley-Rideal reaction between gaseous NO_2 and chemisorbed CO. However, if this would be the case, the same effect should most likely have been observed also for 1% CO, provided the amount of NO_2 is sufficient. For Pt/CeO_2 the decreased activity is likely due to the formation of nitrates and carbonates on the ceria surface that hinder surface diffusion or block active sites on the platinum-ceria boundary.

3.2. Oxidation of CH_4 and $CO+CH_4$ mixture

Figure 5 shows the results from TPO of 0.05% CH_4 over homogeneous (top panel) and heterogeneous (middle panel) Pt/Al_2O_3, and homogeneous and heterogeneous Pt/CeO_2 (bottom panel) during heating-cooling ramps. For the Pt/Al_2O_3 catalysts, the conversion of CH_4 reaches only 10-20% at the top temperature (550°C) studied here.

Contrarily, the Pt/CeO_2 catalysts are rather active showing a light-off temperature of 359 and 385°C for, respectively, the homogeneous and heterogeneous Pt/CeO_2 catalyst. In contrast to the CO oxidation experiments discussed above, the homogeneous catalyst exhibit the lower light-off temperature and no ignition-extinction hysteresis can be observed.

Previous studies have shown that the oxidation of methane over alumina supported platinum is sensitive towards the surface O/Pt ratio [28,29]. The term O/Pt ratio was introduced to account for oxygen in any type of platinum-oxygen species as the IUPAC definitions provide no clear distinction between adsorbed oxygen and platinum oxides [56]. Since in this study, excess oxygen was used in all experiments, the surface O/Pt ratio is expected to be high and thus this is the main explanation to the low methane conversion. For Pt/CeO_2 the situation is obviously different. The O/Pt ratio is expected to be high also in this case, possibly even higher due to the influence of the ceria support on the Pt crystallites. The oxidation of methane over bare ceria is minor even though dissociation of methane may occur [41]. One may consider methane dissociation on ceria with subsequent diffusion of dissociation products to the Pt crystallites where oxidation occurs to explain the results. However, we find this scenario unlikely as methane dissociation probably leads to the formation of various, relatively stable, carbonate- and hydroxyl species on the support. Moreover, the effective oxygen storage function that may drain oxygen from the Pt crystallites through spill-over and further diffusion on/into ceria thereby lowering a detrimentally high surface O/Pt ratio, as suggested for transient studies [40], can hardly explain the present results as continuous oxygen excess was used. Instead we propose, in line with the discussion above, that the Pt/CeO_2 system may provide highly active sites located at the platinum-ceria boundary, that can dissociate methane also under oxygen excess conditions. The reason for the slightly higher activity for the homogeneous catalyst can be a result of the difference in the local Pt loading, i.e., amount of Pt per unit area of support.

We consider now the oxidation of the $CO+CH_4$ mixture. The results for simultaneous oxidation of 1%CO and 0.05%CH_4 over Pt/CeO_2 catalysts are shown in Fig 6. As the ignition- and extinction processes for the two reactions occur in different temperature regions it is tempting to simply treat these as two independent reactions. This is, however, not the case. The CO conversion profiles are shifted to higher temperatures and a reverse ignition-extinction hysteresis (i.e. extinction at higher temperatures than ignition), is observed for the methane oxidation. The oxidation of methane alone shows no such hysteresis, *cf.* Fig 5. The decreased activity for CO oxidation can be due to the blocking of a significant number of the Pt sites by methane dissociation products that cannot be oxidised within this temperature region, so that the CO self-poisoning that eventually occurs during extinction is facilitated. The reversed hysteresis in methane conversion likely originates

from reduction- and oxidation of Pt sites. We recall that the extinction experiment was carried out before the ignition experiment. At the start of the extinction experiment, the surface O/Pt ratio is high and the ceria is in a high oxidation state. The sites mainly responsible for the activity are likely those located at the platinum-ceria boundary as discussed above. During extinction of the oxidation reactions the Pt surface is reduced. As methane dissociation strongly depends on the coverage of other species, the extinction of the methane oxidation likely results in partial reduction of the Pt surface by methane dissociation products. The extinction of the CO oxidation reaction then corresponds to a more complete reduction of the Pt surface. The reduced state, which is more active for methane oxidation, is then the initial condition for the ignition experiment. Consequently, an improved conversion of methane below light-off and lower light-off temperature is seen which in turn results in a reverse ignition-extinction hysteresis. The maximum conversion in the ignition- and extinction experiments occurs at about the same temperature, i.e., the kinetics for the oxidation of the Pt crystallites is sufficiently fast to reach the state where again the sites at the platinum-ceria boundary are mainly responsible for the methane conversion.

4. Concluding remarks

The oxidation of CO, CH_4, and $CO+CH_4$ mixture in excess oxygen over Pt/Al_2O_3 and Pt/CeO_2 catalysts with the platinum phase distributed either homogeneously or heterogeneously in the support material have been studied by temperature programmed experiments. The results show that the catalytic activity follows the order: Pt/CeO_2 (heterogeneous)>Pt/CeO_2 (homogeneous)>Pt/Al_2O_3 (heterogeneous)> Pt/Al_2O_3 (homogeneous) as indicated by lower ignition- and/or extinction temperatures. Also, the influence of NO_2 on the oxidation of CO and CH_4 as well as the influence of CO_2 on CO oxidation were studied. For Pt/Al_2O_3, NO_2 increases the activity for CO oxidation in the pre-ignition regime although the light-off temperature is shifted towards higher temperatures. For methane oxidation over Pt/Al_2O_3 the activity generally increases when NO_2 is added. The addition of CO_2 has minor influence on the activity for CO oxidation. In the case of Pt/CeO_2, the activity for oxidation of CO and CH_4 decreases dramatically in the presence of NO_2. The addition of CO_2 decreases the activity for CO oxidation. For the simultaneous oxidation of CO and CH_4, a reverse hysteresis for methane oxidation is observed, i.e., the extinction process occurs at higher temperature than the corresponding ignition process.

The improved activity for CO oxidation over samples with heterogeneous Pt distribution is likely due to less tendency towards CO self-poisoning through the development of steeper concentration gradients in the Pt containing regions of the porous support material, i.e., the effect of het-

erogeneous Pt distribution is related mainly to mass transport phenomena. This is further supported by the fact that mehane oxidation is not significantly influenced by the heterogeneous Pt distribution. The considerable increase of activity for both reactions over ceria supported Pt is here assigned to highly active sites at the platinum-ceria boundary but also, to some extent, the oxygen storage- and release function and dynamics of the transport of oxygen in the Pt/CeO_2 system.

5. Acknowledgments

References

[1] P. Gélin, M. Primet, Appl. Catal. B: Environ. 39 (2002) 1-37.

[2] R. M. Heck and R. J. Farrauto, Appl. Catal. A: General 221 (2001) 443-57.

[3] H. S. Gandhi, G. W. Graham and R. W. McCabe, J. Catal. 216 (2003) 433-42.

[4] G. Lenaers, Sci. Total. Environ. 190 (1996) 139-47.

[5] M. Skoglundh, E. Fridell, Top. Catal. 28(1-4) (2004) 79-87.

[6] S. A. Lewis, J. M. E. Storey, B. Bunting, J. P. Szybist, SAE technical paper series 2005-01-3737.

[7] S. V. Bohac, M. Han, T. J. Jacobs, A. J. López, D. N. Assanis, SAE technical paper series 2005-01-3737.

[8] J. Wei, Adv. Catal. 24 (1975) 57-129.

[9] G. Ertl, T. Engel, Adv. Catal. 28 (1979) 1-77.

[10] M. Bär, Ch. Zülicke, M. Eiswirth and G. Ertl, J. Chem. Phys. 96(11) (1992) 8595-8604.

[11] V. P. Zhdanov and B. Kasemo, Surf. Sci. Rep. 20 (1994) 111-89.

[12] S. Salomons, R. E. Hayes, M. Votsmeier, A. Drochner, H. Vogel, S. Malmberg and J. Gieshoff, Appl. Catal. B: Environ. 70 (2007) 305-13.

[13] P.-A. Carlsson, M. Skoglundh, E. Fridell, E. Jobson and B. Andersson, Catal. Today. 73 (2002) 307-13.

[14] P.-A. Carlsson, M. Skoghlundh, P. Thormählen and B. Andersson, Top. Catal. 30/31 (2004) 375-81.

[15] P.-A. Carlsson, V. P. Zhdanov and M. Skoghlundh, Phys. Chem. Chem. Phys. 8 (2006) 2703-6.

[16] S. Bernal, J. J. Calvino, M. A. Cauqui, J. M. Gatica, C. Larese, J. A. Pérez Omil and J. M. Pintado, Catal. Today 50 (1999) 175-206.

[17] L. F. Liotta, A. Longo, A. Macaluso, A. Martorana, G. Pantaleo, A. M. Venezia and G. Deganello, Appl. Catal. B: Environ. 48 (2004) 133-49.

[18] J. Libuda, H.-J. Freund, Surf. Sci. rep. 57 (2005) 157-298.

[19] V. P. Zhdanov and B. Kasemo, J. Catal. 170 (1997) 377-89.

[20] P.-A. Carlsson, L- Österlund, P. Thormählen, A. Palmqvist, E. Fridell, M. Skoglundh, J. Catal. 226 (2004) 422-34.

[21] P.-A. Carlsson, V. P. Zhdanov, B. Kasemo, Appl. Surf. Sci. 239 (2005) 424-31.

[22] R. Burch and M. J. Hayes, J. Mol. Catal. A: Chemical, 100 (1995) 13-33.

[23] R. Burch, D. J. Crittle, M. J. Hayes, Catal. Today. 47 (1999) 229-34.

[24] S. Oh, P. J. Mitchell and R. M. Siewert, J. Catal. 132 (1991) 287-310.

[25] P.-A. Carlsson, S. Mollner, K. Arnby, M. Skoglundh, Chem. Sci. Eng. 59 (2004) 4313-23.

[26] K. Arnby, J. Assiks, P.-A. Carlsson, A. Palmqvist, M. Skoglundh, J. Catal. 233 (2005) 176-85.

[27] P.-A. Carlsson, E. Fridell, M. Skoglundh, Catal. Lett. 115(1-2) (2007) 1-7.

[28] E. Becker, P.-A. Carlsson, H. Grönbeck, M. Skoglundh, J. Catal. 252 (2007) 11-17.

[29] E. Becker, P.-A. Carlsson, L. Kylhammar, M. Newton and M. Skoglundh, J. Phys. Chem. C (2010).

[30] P.-A. Carlsson, M. Nordström and M. Skoglundh, Top. Catal. 52 (2009) 1962-66.

[31] V. P. Zhdanov, P.-A. Carlsson, B. Kasemo, J. Chem. Phys. 126 (2007) 234705.

[32] H. C. Yao and Y. Y.-F. Yao, J. Catal. 86 (1984) 254-65.

[33] E. C. Sue, C.N. Montreuil and W. G. Rothchild, Appl. Catal. 17 (1985) 75-86.

[34] J. S. Rieck and A. T. Bell, J. Catal. 99 (1986) 278-92.

[35] G. Kim, Ind. Eng. Chem. Prod. Res. Dev. 21 (1982) 267-74.

[36] H. S. Gandhi and M. Shelef,, "Catalysis and Automotive Pollution Control", A. Crucq and A. Frennet (Editors), 1987, pp. 199-214.

[37] H.C. Yao, Appl. Surf. Sci. 19 (1984) 398-406.

[38] S. Johansson, L. Österlund, B. Kasemo, J. Catal. 201 (2001) 275-85.

[39] E. Becker, P. Thormählen, T. Maunula, A. Suopanki and M. Skoglundh, Top. Catal. 42/43 (2007) 421-24.

[40] E. Becker, P.-A. Carlsson and M. Skoglundh, Top. Catal. 52 (2009) 1957-61.

[41] E. Odier, Y. Schuurman and C. Mirodatos, Catal. Today 127 (2007) 230-37.

[42] K. Arnby, A. Törncrona, B. Andersson, M. Skoglundh, J. Catal. 221 (2004) 252-61.

[43] S. Bernal, J. J. Calvino, J. M. Gatica, C. L. Cartes and J. M. Pintado, "Catalysis by ceria and related materials". A. Trovarelli (Editor), 2002, pp. 85-167.

[44] P. Ericsson, M. Holmström, A. Amberntsson-Carlsson C. Ohlson, M. Skoglundh, B. Andersson and P.-A. Carlsson, SAE technical paper series 2007-01-1746.

[45] P. B. Weisz and C. D. Prater, Adv. Catal. 6 (1954) 143-96.

[46] P. B. Weisz, Z. Physik. Chem., Neue Folge, 11 (1957) 1.

[47] D. E. Mears. Ind. Eng. Chem. Process. Des. Develop. 10(4) (1971) 541- 47.

[48] D. A. Frank-Kamenetskii, "Diffusion and heat transfer in chemical kinetics", Plenum press, New York, 1969, p. 487.

[49] A. Schwartz, L. L. Holbrook and H. Wise, J. Catal. 21 (1971) 199-207.

[50] S. Y. Joshi, M. P. Harold and V. Balakotaiah, Chem. Eng. Sci. 65 (2010) 1729-47.

[51] A. Trovarelli, Catal. Rev. Sci. Eng. 38 (1996) 439-520.

[52] D. Martin and D. Duprez, J. Phys. Chem. 100 (1996) 9429-38.

[53] P. Bazin, O. Sour, J. C. Lavalley, M- Daturi and G. Blanchard, Phys. Chem. Chem. Phys. 7 (2005) 187-94.

[54] Y. Lykhach, T. Staudt, M. P. A. Lorenz, R. Streber, A. Bayer, H.-P. Steinrück and J. Libuda, Chem. Phys. Chem. 11 (2010) 1496-1504.

[55] E. Aneggi, J. Llorca, M. Boaro and A. Trovarelli, J. Catal. 234 (2005) 88-95.

[56] R. Burwell, Adv. Catal. 26 (1977) 351-93.

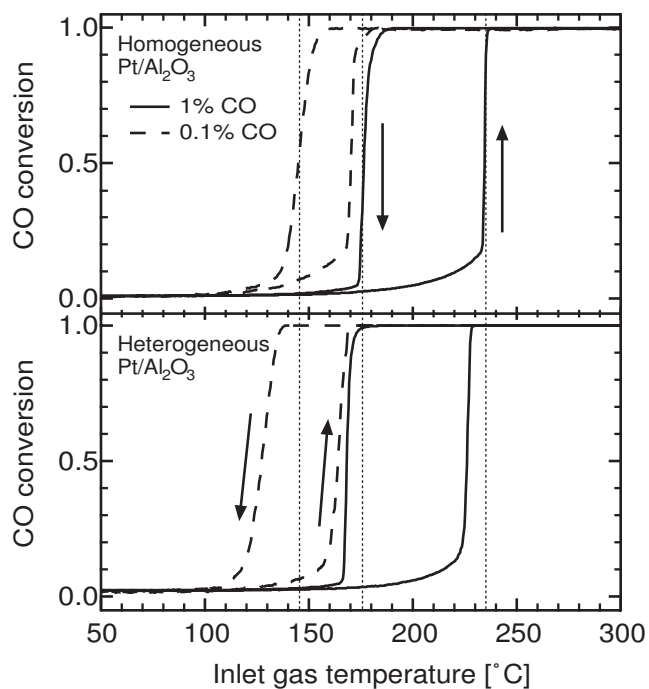Fig. 1. Temperature programmed oxidation of 0.1 and 1% CO with 9% O_2 over homogeneous (top panel) and heterogeneous (bottom panel) Pt/Al_2O_2 monolith catalysts using heating/cooling rates of 5°C/min.
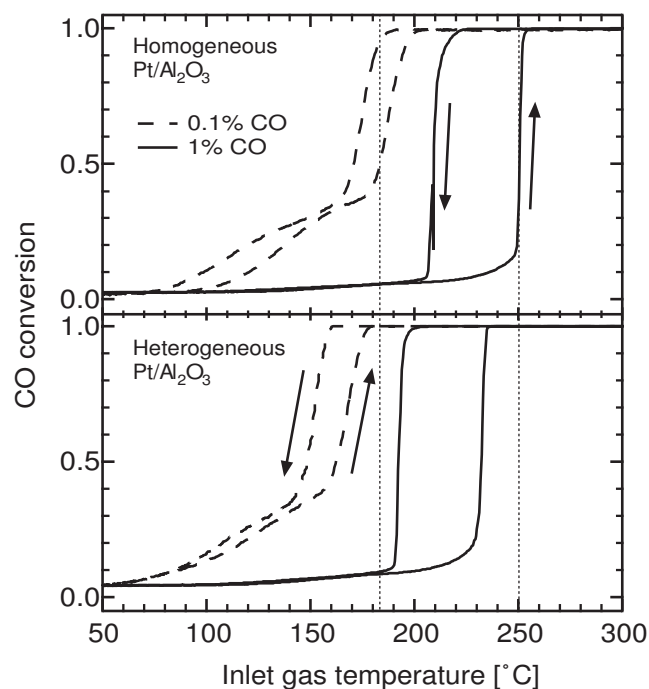

Fig. 3. Temperature programmed oxidation of 0.1 and 1% CO with 9% O_2 in the presence of 0.03% NO_2 over homogeneous (top panel) and heterogeneous (bottom panel) Pt/Al_2O_2 monolith catalysts using heating/cooling rates of 5°C/min.
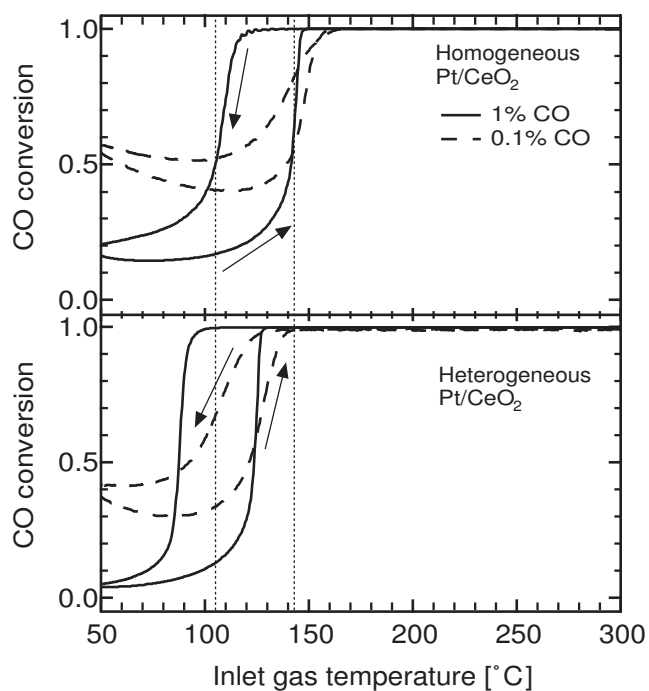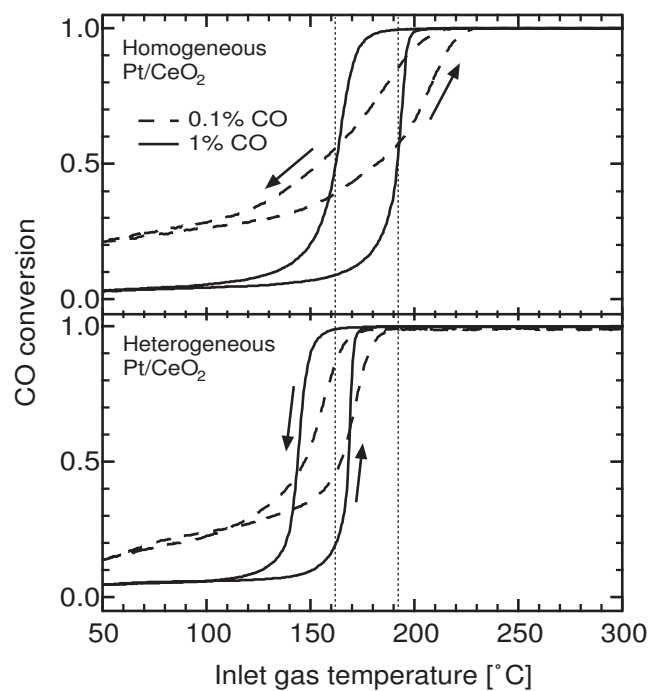

Fig. 2. Temperature programmed oxidation of 0.1 and 1% CO with 9% O_2 over homogeneous (top panel) and heterogeneous (bottom panel) Pt/CeO_2 monolith catalysts using heating/cooling rates of 5°C/min.

Fig. 4. Temperature programmed oxidation of 0.1 and 1% CO with 9% O_2 in the presence of 0.03% NO_2 over homogeneous (top panel) and heterogeneous (bottom panel) Pt/CeO_2 monolith catalysts using heating/cooling rates of 5°C/min.
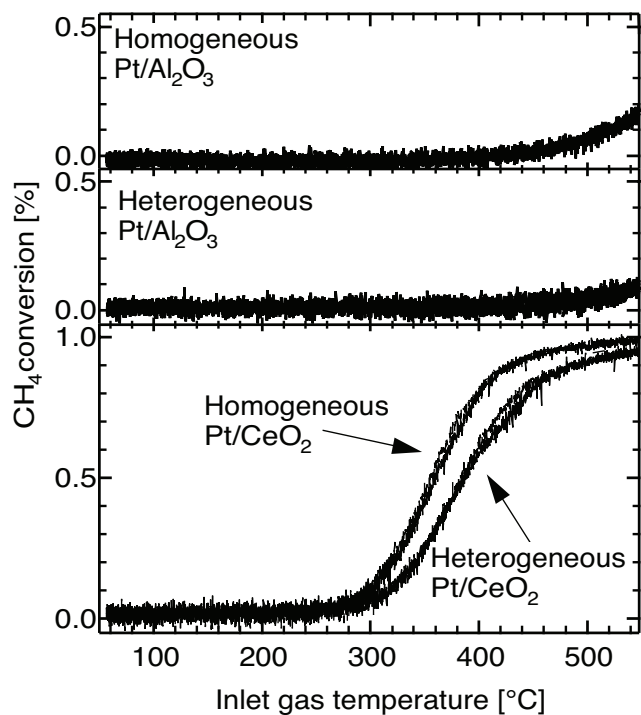
Fig. 5. Ignition and extinction of oxidation of CH_4 over homogeneous and heterogeneous Pt/Al_2O_2 monolith catalysts (top and middle panel respectively) and the corresponding Pt/CeO_2 catalysts (bottom panel).
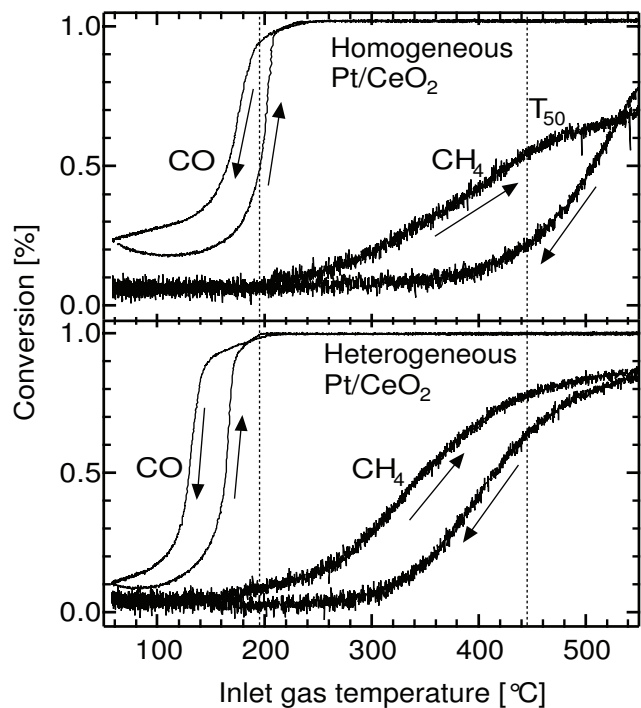

Fig. 6. Ignition and extinction of oxidation of $CO+CH_4$ over homogeneous (top panel) and heterogeneous (bottom panel) Pt/CeO_2 monolith catalysts.

9